© 2017. Published by The Company of Biologists Ltd | Journal of Experimental Biology (2017) 220, 775-786 doi:10.1242/jeb.148429

RESEARCH ARTICLE

Different mechanisms of Na^+ uptake and ammonia excretion by the gill and yolk sac epithelium of early life stage rainbow trout

Alex M. Zimmer[1,2,3,*], Jonathan M. Wilson[2], Patricia A. Wright[4], Junya Hiroi[5] and Chris M. Wood[3]

ABSTRACT

In rainbow trout, the dominant site of Na^+ uptake ($J_{Na,in}$) and ammonia excretion (J_{amm}) shifts from the skin to the gills over development. Post-hatch (PH; 7 days post-hatch) larvae utilize the yolk sac skin for physiological exchange, whereas by complete yolk sac absorption (CYA; 30 days post-hatch), the gill is the dominant site. At the gills, $J_{Na,in}$ and J_{amm} occur via loose Na^+/NH_4^+ exchange, but this exchange has not been examined in the skin of larval trout. Based on previous work, we hypothesized that, contrary to the gill model, $J_{Na,in}$ by the yolk sac skin of PH trout occurs independently of J_{amm}. Following a 12 h exposure to high environmental ammonia (HEA; 0.5 mmol l^{-1} NH_4HCO_3; 600 µmol l^{-1} Na^+; pH 8), J_{amm} by the gills of CYA trout and the yolk sac skin of PH larvae, which were isolated using divided chambers, increased significantly. However, this was coupled to an increase in $J_{Na,in}$ across the gills only, supporting our hypothesis. Moreover, gene expression of proteins involved in $J_{Na,in}$ [Na^+/H^+-exchanger-2 (NHE2) and H^+-ATPase] increased in response to HEA only in the CYA gills. We further identified expression of the apical Rhesus (Rh) proteins Rhcg2 in putative pavement cells and Rhcg1 (co-localized with apical NHE2 and NHE3b and Na^+/K^+-ATPase) in putative peanut lectin agglutinin-positive (PNA^+) ionocytes in gill sections. Similar Na^+/K^+-ATPase-positive cells expressing Rhcg1 and NHE3b, but not NHE2, were identified in the yolk sac epithelium. Overall, our findings suggest that the mechanisms of $J_{Na,in}$ and J_{amm} by the dominant exchange epithelium at two distinct stages of early development are fundamentally different.

KEY WORDS: Larval fish, PNA^+ ionocyte, Na^+/H^+-exchanger, NHE, Rhesus glycoproteins, Ion regulation

INTRODUCTION

The relationship between sodium uptake ($J_{Na,in}$) and ammonia excretion (J_{amm}) by freshwater fish has been a focus of comparative physiologists for over seven decades. August Krogh (1939) first suggested that the excretion of NH_4^+ is tied to the active uptake of Na^+ across the fish gill and this topic has since been studied extensively (see Wilkie, 1997, 2002; Weihrauch et al., 2009; Ip and Chew, 2010; Wright and Wood, 2009, 2012, for reviews). In most mature freshwater fish, $J_{Na,in}$ and J_{amm} occur primarily across the gills (Smith, 1929; Maetz and Garcia-Romeu, 1964; Cameron and Heisler, 1983; Wright and Wood, 1985; Smith et al., 2012; Zimmer et al., 2014a), although the skin, kidney, and gastrointestinal system play minor roles. However, in post-hatch larval fish, the gills are underdeveloped and the skin (primarily that overlying the yolk sac) represents the dominant site for both $J_{Na,in}$ and J_{amm} (Esaki et al., 2007; Shih et al., 2008; Fu et al., 2010; Zimmer et al., 2014c).

Recent work in ionoregulatory physiology has pointed towards multiple species-specific models for Na^+ uptake by freshwater fish (see Dymowska et al., 2012, for review). In rainbow trout, a portion of branchial $J_{Na,in}$ occurs as coupled Na^+/NH_4^+ exchange (Wright and Wood, 2009; Weihrauch et al., 2009) via a complex involving Rhesus (Rh) glycoproteins that function as ammonia-conductive channels (Nakada et al., 2007; Nawata et al., 2007; Nawata et al., 2010). In this complex, $J_{Na,in}$ across apical surfaces of ionocytes is effected by Na^+/H^+-exchangers (NHEs) and Na^+ channels coupled to electrogenic H^+-ATPases. Studies in zebrafish have directly demonstrated a role for NHEs in $J_{Na,in}$ whereby a functional metabolon is formed with an apical Rh glycoprotein (Rh-NHE metabolon) (Kumai and Perry, 2011; Shih et al., 2012). In this metabolon, Rh proteins transport ammonia from the cytosol to the apical boundary layer by binding NH_4^+, stripping off a proton, and conducting NH_3 (Nawata et al., 2010; Caner et al., 2015; see Wright and Wood, 2012, for review); these protons then drive Na^+/H^+ exchange by NHE. H^+-ATPase also plays a part in Na^+/NH_4^+ exchange by simultaneously driving electrogenic $J_{Na,in}$ via putative Na^+ channels, which are potentially acid-sensing ion channels (ASICs) (Dymowska et al., 2014), and promoting apical boundary layer acidification that facilitates apical acid-trapping of NH_3 (see Wright and Wood, 2012, for review). The current model of Na^+/NH_4^+ exchange in trout suggests that the NHE mechanism is localized to a subset of mitochondrion-rich cells or ionocytes that bind peanut agglutinin lectin (PNA^+ ionocytes), whereas the H^+-ATPase mechanism is localized to ionocytes that do not bind PNA (PNA^- ionocytes) (see Dymowska et al., 2012, for review).

Presently, no transport model exists for $J_{Na,in}$ or J_{amm} by the yolk sac epithelium of rainbow trout. In zebrafish, several studies have established a model of Na^+ transport by the yolk sac skin. Cutaneous $J_{Na,in}$ by the yolk sac skin of larval zebrafish is coordinated by NHE (NHE3b) and H^+-ATPase (Lin et al., 2006; Esaki et al., 2007; Kumai and Perry, 2011; Shih et al., 2012; Ito et al., 2013), and Rh proteins also play an integral role in J_{amm} in larval zebrafish (Nakata et al., 2007; Shih et al., 2008; Braun et al., 2009). However, under high Na^+ concentration ([Na^+]; 0.5–0.8 mmol l^{-1}) and high pH (pH 7–8) conditions there does not seem to be coupling between $J_{Na,in}$ and J_{amm} by the yolk sac epithelium of zebrafish. Kumai and Perry (2011) demonstrated that only larvae reared under low pH (pH 4) display functional coupling between $J_{Na,in}$ and J_{amm}, mediated by NHE3b and Rhcg1. Shih et al. (2012) observed the same phenomenon in zebrafish larvae reared in low [Na^+] (0.05 mmol l^{-1}).

[1]Department of Biology, University of Ottawa, Ottawa, ON, Canada K1N 6N57. [2]Department of Biology, Wilfrid Laurier University, ON, Canada N2L 3C5. [3]Department of Zoology, University of British Columbia, Vancouver, BC, Canada V6T 1Z4. [4]Department of Integrative Biology, University of Guelph, Guelph, ON, Canada N1G 2W1. [5]Department of Anatomy, St Marianna University School of Medicine, Miyamae, Kawasaki 216-8511, Japan.

*Author for correspondence (azimmer@uottawa.ca)

A.M.Z., 0000-0002-4574-1334

Received 17 August 2016; Accepted 7 December 2016

Journal of Experimental Biology (2017) 220, 775-786 doi:10.1242/jeb.148429

In larval rainbow trout, Rh gene expression increases with increasing $J_{Na,in}$ and J_{amm} over development (Hung et al., 2008; Zimmer et al., 2014c), and transcripts for Rhcg1, Rhcg2 and Rhbg have been detected in both the yolk sac skin and body skin of larval trout (Zimmer et al., 2014c). Little is known, however, regarding the functional mechanisms of $J_{Na,in}$ or J_{amm} by the yolk sac skin of post-hatch trout. Does the model resemble that of the trout gill (flexible Na^+/NH_4^+ exchange under high [Na^+] or high pH conditions) or that of the zebrafish yolk sac epithelium (Na^+/NH_4^+ exchange present only under low [Na^+] or low pH conditions)?

The goal of the present study was to establish mechanistic models for $J_{Na,in}$ and J_{amm} by the dominant exchange epithelium of two distinct stages of early development in trout: the yolk sac skin of post-hatch larvae (PH; 7 days post-hatch) and the gills of trout that have completed yolk sac absorption (CYA; 30 days post-hatch). Our hypothesis was that the mechanisms of $J_{Na,in}$ and J_{amm} differ between the gills and yolk sac epithelium of early life stage trout, based on earlier work that showed a strong correlation between branchial $J_{Na,in}$ and J_{amm} over post-hatch development in rainbow trout and a lack thereof at the skin (Zimmer et al., 2014c). Moreover, we aimed to determine whether the transport mechanisms utilized by the gills of CYA trout are similar to those described for juvenile and adult trout upon which the current branchial model is based (see Wright and Wood, 2009 and Dymowska et al., 2012 for review).

Two different divided chambers were used to assess $J_{Na,in}$ and J_{amm} by the gills of CYA trout and yolk sac skin of PH trout under control conditions and following exposure to high environmental ammonia (HEA), a treatment that has been previously shown to upregulate components of the Na^+/NH_4^+ exchange complex in the gills of adult and juvenile trout (Nawata et al., 2007; Tsui et al., 2009; Zimmer et al., 2010; Wood and Nawata, 2011; Sinha et al., 2013). We predicted that there would be significant Na^+/NH_4^+ exchange by the CYA gills whereas J_{amm} and $J_{Na,in}$ by the PH yolk sac skin would occur independently (Zimmer et al., 2014c). We additionally assessed transport across the general body skin of CYA trout. Changes in gene expression of several components of the Na^+/NH_4^+-exchange complex (Rh proteins, NHE, H^+-ATPase) in response to HEA exposure in the CYA gill and body skin and the PH yolk sac skin were quantified, and immunostaining of several proteins potentially involved in the Na^+/NH_4^+ exchange complex was conducted. The effects of specific pharmacological blockers (EIPA for NHE; bafilomycin for H^+-ATPase; phenamil for putative Na^+ channels) on branchial and cutaneous fluxes were also examined. The overall findings of this study have been summarized in two mechanistic models describing $J_{Na,in}$ and J_{amm} across the CYA gill and PH yolk sac.

MATERIALS AND METHODS

Fish

Rainbow trout *Oncorhynchus mykiss* (Walbaum 1792) embryos were purchased from Rainbow Springs Hatchery (Thamesford, ON, Canada) in the eyed stage and reared at 12°C in flow-through dechlorinated tap water from Hamilton, ON, Canada (moderately hard: [Na^+]=0.6 mmol l^{-1}, [Cl^-]=0.8 mmol l^{-1}, [Ca^{2+}]=0.8 mmol l^{-1}, [Mg^{2+}]=0.15 mmol l^{-1}, [K^+]=0.05 mmol l^{-1}; titration alkalinity 2.1 mequiv l^{-1}; pH ~8.0; hardness ~140 g l^{-1} as $CaCO_3$ equivalents). Embryos hatched ~1 week after purchase [post-hatch (PH) larvae] and complete yolk sac absorption (CYA) occurred 30 days thereafter. Following CYA, fish were fed a daily ration of commercial trout pellets (Martin Profishent Aquaculture Nutrition, Tavistock, ON, Canada; 45% crude protein, 9% crude fat, 3.5% crude fiber) of ~5% body mass. In all experiments, CYA larvae were fasted for at least 24 h prior to experimentation. All procedures were approved by the McMaster University Animal Research Ethics Board (AUP 12-12-45) and adhered to the guidelines of the Canadian Council on Animal Care.

Divided chamber design

The designs of both divided chambers used in the present study are illustrated in Fig. 1. The first or 'traditional' divided chamber (Fig. 1A) was designed to separate the head and gills from the rest of the body in CYA fish (Fu et al., 2010) and the protocol was almost identical to those described in previous studies (Zimmer et al., 2014c; Zimmer and Wood, 2015). CYA trout (~200 mg; 30 days post-hatch) were initially anaesthetized to stage 3 anesthesia (McFarland, 1959) using 0.1 g l^{-1} neutralized MS-222 with 0.05 g l^{-1} neutralized MS-222 used to maintain anesthesia in the chambers. Fluxes of ammonia and Na^+ across the gill epithelium were assessed in the anterior chamber (Series 1 and 3), whereas fluxes across the body epithelium were assessed in the posterior chamber (Series 1 only).

The second type of divided chamber (Fig. 1B) was designed to isolate the yolk sac of post-hatch (PH) larvae from the rest of the body. At 5–7 days post-hatch, the stage at which PH larvae

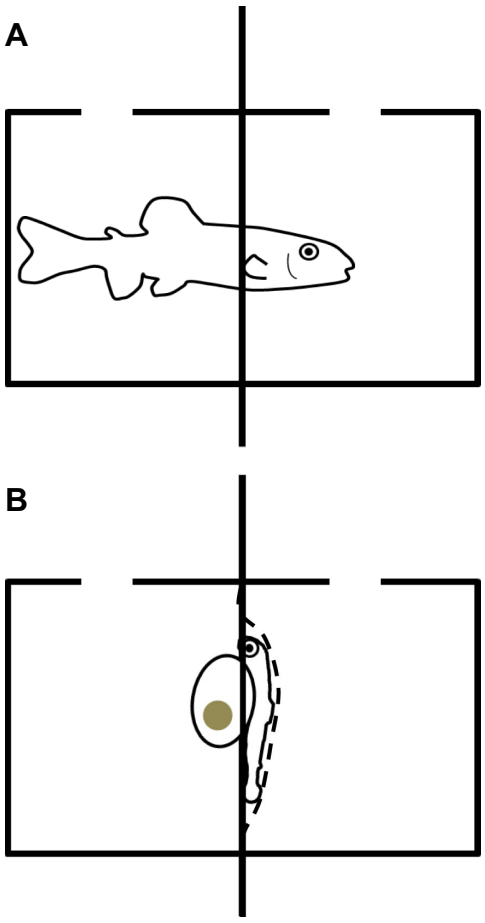

Fig. 1. Schematic diagrams of divided chambers. Schematic diagram of (A) 'traditional' divided chamber used to assess flux across the gill and body of complete yolk sac absorption (CYA)-stage trout and (B) divided chamber used to assess flux across the yolk sac of 7 days post-hatch (PH) larvae. Vertical line across the chambers indicates a latex dam separating the two sections, and dotted line in B indicates the additional perforated latex sheet securing the embryo in place.

Journal of Experimental Biology

Journal of Experimental Biology (2017) 220, 775-786 doi:10.1242/jeb.148429

(~80 mg) were easiest to handle, randomly selected larvae were anesthetized using 0.2 g l^{-1} neutralized MS-222. Larvae were then loaded into divided chambers containing 0.05 g l^{-1} neutralized MS-222 to maintain anesthesia. The yolk sac of the larva was pushed through a small hole (~3–4 mm) in the center of a thin latex dam such that it was spatially separated from the rest of the body. A second perforated latex sheet (dashed line in Fig. 1B) was placed over the dorsal side of the fish to help secure the larva in place. The larva, secured between the latex dams, was then mounted between two 5-ml half-chambers such that the fish was positioned laterally with its dorsal side (body and head) contained within one chamber and its ventral side (yolk sac) contained within the other. Flux across the yolk sac epithelium was assessed in the ventral chamber (Series 1 and 3).

Experimental series

Series 1

This series evaluated the presence or absence of Na^+-coupled J_{amm} by the CYA gill and body epithelia and the PH yolk sac epithelium in response to ammonia loading. CYA fish or PH larvae were exposed to either control conditions or to high environmental ammonia (HEA; 0.5 mmol l^{-1} NH_4HCO_3) for 12 h in a 3-litre static exposure containing ~15 fish. After 12 h, fish were loaded individually into respective divided chamber systems (Fig. 1) containing ammonia-free water and air lines were placed in both chambers. Larvae were allowed to adjust to this setup for 30 min before 0.5 µCi of ^{22}Na (Perkin Elmer, Waltham, MA, USA) was added to one chamber (volume=5 ml). For CYA fish, the radioisotope was added to the anterior chamber for gill fluxes or the posterior chamber for body epithelium fluxes; for PH larvae, the radioisotope was added only to the ventral chamber for yolk sac epithelium fluxes. Following 5 min of mixing, an initial 1.25-ml sample was taken from the isotope-loaded chamber. Fluxes lasted 1 h; a final 1.25-ml sample was taken from the same chamber and a 0.25-ml sample was also taken from the unloaded chamber to check for leaks across the dam. The fish was then removed and rinsed in radioisotope-free water for 5 min, during which time they were monitored to assess recovery from anesthesia. In all experiments, radioisotope leak was less than 10%, and fish fully recovered from anesthesia within 5 min, following which they were euthanized via neutralized MS-222 overdose. Final chamber volume was recorded and then larvae were weighed and counted to determine ^{22}Na gamma-radioactivity (see 'Analytical Procedures', below). Aliquots (0.25 ml) of all samples were stored at 4°C for later determination of ^{22}Na gamma-radioactivity and total [Na^+]. The remaining 1 ml was stored at −20°C for later analysis of total ammonia concentration (T_{amm}).

Series 2

In Series 2, the response to HEA exposure at the gene and protein levels was assessed. Randomly selected PH and CYA larvae were exposed to either control conditions or to HEA (0.5 mmol l^{-1} NH_4HCO_3) for 12 h under the same conditions as described above. Following the exposure, half of the fish were removed from each treatment and euthanized in a solution containing the respective NH_4HCO_3 concentration and a lethal dose of neutralized MS-222. Fish were then transferred individually into vials containing 20 ml of 10% neutral buffered formalin and were fixed overnight at 4°C. Fixed fish were then transferred individually into vials containing 20 ml of 70% ethanol for 24 h at 4°C, after which the ethanol solution was replaced with a formic acid–sodium citrate solution (35% formic acid; 13% w/v sodium citrate) for decalcification, which eased sectioning of fish. Larvae were decalcified for 48 h at 4°C and then transferred again to 70% ethanol and stored at 4°C.

The remaining fish were euthanized individually following the same protocol and gill and body skin (CYA fish) and yolk sac skin (PH fish) were dissected and collected under a dissecting microscope. Tissue samples were immediately snap-frozen individually in liquid nitrogen and stored at −80°C. All dissections were conducted in the respective treatment water (containing a lethal dose of neutralized MS-222) held at 12°C and were completed within 2–3 min following euthanasia for each individual fish.

Series 3

The third experimental series was designed to determine the effects of various pharmacological blockers on fluxes by the CYA gill and PH yolk sac epithelium. The protocol for this series followed that described for Series 1 except for some minor changes as follows. For CYA fish, only flux across the gills was assessed, as Series 1 experiments demonstrated that the body skin contributed minimally to overall $J_{Na,in}$, and there was no evidence of linkage to J_{amm} (see Results, Series 1, below). Also for CYA fish, both control fish and those exposed to HEA for 12 h were tested; for PH larvae, only control fish were tested as HEA did not alter $J_{Na,in}$ by the yolk sac skin (see Results, Series 1, below). Furthermore, only $J_{Na,in}$ could be assessed in the PH divided chambers owing to the methodological limitations of the ammonia assay in the presence of 0.1% DMSO (see 'Analytical procedures', below).

Immediately after the fish were loaded into divided chambers, 5 µl of DMSO (vehicle) containing the relevant blocker was added to the same chamber that would later receive the addition of ^{22}Na, such that the final concentration of DMSO was 0.1%. The blockers (and final concentrations) used were 5-(*N*-ethyl-*N*-isopropyl)amiloride (EIPA; Sigma, St Louis, MO, USA; 1×10^{-4} mol l^{-1}), bafilomycin (Cayman Chemical, Ann Arbor, MI, USA; 5×10^{-6} mol l^{-1}), and phenamil (Cayman Chemical, Ann Arbor, MI, USA; 1×10^{-4} mol l^{-1}), which targeted NHEs, H^+-ATPase, and epithelial Na^+ channels, respectively. Following the addition of these blockers (or 0.1% DMSO alone as a vehicle control), fish were left for 30 min to allow blocker effects to develop. The remainder of the experiment followed the same protocol described above for Series 1.

Analytical procedures

$J_{Na,in}$ and J_{amm}

^{22}Na gamma radioactivity (counts per minute; cpm) in water samples and whole larvae was measured by gamma counting (Perkin Elmer Wizard 1480 3″ Auto Gamma Counter, Waltham, MA, USA), and [Na^+] of water samples was determined by atomic absorption spectrophotometry (Varian SpectrAA 220FS Atomic Absorption Spectrophotometer, Palo Alto, CA, USA). T_{amm} in water samples was measured using the protocol outlined by Verdouw et al. (1978). Note that in Series 3, samples were compared against T_{amm} standards prepared in the same DMSO concentration and/or blocker concentration present in the particular treatment water. This was necessary as each of the DMSO and the blocker/DMSO combinations differentially decreased the sensitivity, but not the linearity, of the assay. To assess the sensitivity of the T_{amm} assay in the presence of 0.1% DMSO, the method detection limit (MDL) was determined. We aimed to determine the lowest change in T_{amm} that could reliably be measured by the assay. As such, MDL was calculated by measuring ten 5 µmol l^{-1} and 10 µmol l^{-1} standards, determining the standard deviation of the difference between these 10 standards, and multiplying the standard deviation by 3, which is

an approximation of the critical value of the t distribution for a sample size with 9 degrees of freedom. The MDL for the assay in the presence of DMSO was 7 µmol l^{-1}, indicating that this was the lowest change in T_{amm} that could be reliably detected using this method. Given that changes in T_{amm} in the PH divided chambers were only ~5–10 µmol l^{-1}, we could not accurately determine differences in J_{amm} by the yolk sac skin in response to DMSO and blocker treatments. In CYA fish, however, changes in T_{amm} were >30 µmol l^{-1} and we were able to reliably assess the effects of DMSO and the pharmacological blockers on branchial J_{amm} in this instance. $J_{Na,in}$ and J_{amm} were calculated as previously described (Zimmer et al., 2014c). Note that in previous studies on larvae utilizing similar divided chambers (Fig. 1A) (Fu et al., 2010; Zimmer et al., 2014c) anterior flux rates were corrected to account for cutaneous contributions of the skin localized to the anterior chamber. In the present study, we opted to forego this correction as we could not be certain that our treatments affected branchial and cutaneous fluxes equally. For clarity, we hereafter refer to anterior and posterior fluxes in CYA fish as branchial and cutaneous fluxes, respectively.

Quantitative PCR (qPCR)

Frozen tissue samples were placed in 600 µl of ice-cold lysis buffer (PureLink RNA mini kit, Ambion, Austin, TX, USA) and homogenized for 30 s using a motorized homogenizer (PowerGen 125 homogenizer, Fisher Scientific, Toronto, ON, Canada). RNA was extracted using the PureLink RNA mini kit (Ambion); DNase treatment (Ambion) was performed on-column. RNA concentration and purity were determined spectrophotometrically (Nanodrop ND-1000; Nanodrop Technologies, Wilmington, DE, USA) and RNA quality was assessed by running samples on a 1% agarose gel using Redsafe (FroggaBio, North York, ON, Canada) staining. cDNA was synthesized from 200 ng of RNA using an oligo(dT_{17}) primer and superscript II reverse transcriptase (Invitrogen, Carlsbad, CA, USA). qPCR was performed on cDNA samples using previously validated primers (Nawata et al., 2007; Hung et al., 2008; Ivanis et al., 2008; Wood and Nawata, 2011); reaction volume was 10 µl and consisted of 4 µl diluted template cDNA, 5 µl 2× SsoFast EvaGreen Supermix (Bio-Rad, Hercules, CA, USA), and 4 pmol each of forward and reverse primers. Reactions were performed in 96-well plates in a CFX Connect real-time PCR detection system (Bio-Rad) at 98°C for 2 min to initially activate the polymerase enzyme, followed by 40 cycles of 2 s at 98°C and 5 s at 60°C. Melt curve analysis was performed to ensure a single amplification product. No-template controls were performed on every plate and a non-reverse-transcribed control was performed for every primer pair. Reaction efficiency for every primer pair was between 90–110% and mRNA expression of target genes was normalized using the geometric mean of EF1α and β-actin mRNA expression. Stable reference gene pair expression was confirmed by coefficient of variation and expression stability (M) values below the CFX software thresholds of 0.25 and 0.5, respectively. Gene expression in gill and skin tissues from control and HEA-exposed fish was expressed relative to control mean values in each tissue.

Immunohistochemistry

Fixed and decalcified whole larvae were cut into four sections along the length of the fish and processed for paraffin embedding. This was necessary to fit the fish into the paraffin blocks and to allow cross-sectioning through different regions of the fish. Paraffin blocks were sectioned at a thickness of 5 µm and mounted onto aminopropylsilane-coated glass slides. Sections were then dewaxed and antigen retrieval was performed in 0.05% citraconic anhydride (pH 7.3; 30 min at 100°C). Primary antibodies used for probing were: rabbit anti-Rhcg1 (1:500; this study), rabbit anti-Rhcg2 (1:100; this study), rabbit anti-Rhbg (1:100; this study), rabbit anti-NHE2 (N2R15; 1:100; Ivanis et al., 2008), rabbit anti-NHE3b (1:200; this study), and mouse anti-Na^+/K^+-ATPase (α5; 1:100; Takeyasu et al., 1988). For NHE3b, rabbit polyclonal antiserum was raised against a cocktail of synthetic peptides corresponding to two regions of rainbow trout NHE3b (position 755–769: GDEDFEFSEGDSASG; 818–839: PSQRAQLRLPWTPSNLRRLAPL) and were purified by affinity chromatography. The antisera for Rhcg1, Rhcg2 and Rhbg were raised against synthetic peptides corresponding to rainbow trout Rhcg1 (454–467: PEDEENNPPTVEYN), Rhcg2 (475–487: MIHKRQDLSESNF) and Rhbg (448–461: TTVRTPDEAEKLNA), respectively, and were also purified by affinity chromatography. Peptide synthesis, antibody production, and affinity purification were conducted by Eurofins Genomics (Tokyo, Japan). Specificity of the antibodies for NHE3b and Rh proteins were confirmed by a pre-absorption test in gill sections collected from a separate group of juvenile rainbow trout.

The triple-labeling procedure of larval sections was conducted as follows. Sections blocked with 5% normal goat serum for 20 min at room temperature were then incubated with first rabbit primary antibody and the monoclonal α5 antibody at the dilutions given above, overnight at 4°C. Sections were then incubated with the first secondary antibody, which was a goat anti-rabbit Alexa 647-conjugated fragment antigen-binding (Fab) fragment (1:500; no. 111-607-003, Jackson ImmunoResearch, West Grove, PA, USA) for 1 h at 37°C. Sections were then blocked with unlabeled Fab fragment (1:100; no. 111-007-003, Jackson ImmunoResearch) for 1 h at 37°C followed by rinses and incubation with the second rabbit primary antibody at the dilution listed above for 1 h at 37°C. Sections were rinsed and incubated with second secondary antibodies, goat anti-rabbit Alexa Fluor 488 (1:500; no. 711-545-152, Jackson ImmunoResearch) and goat anti-mouse Alexa Fluor 555 (1:500; ab150114, Abcam, Toronto, ON, Canada), for 1 h at 37°C. Note that Rhbg was labeled using only one primary labeling step instead of two, as a simple double-labeling procedure (1 h primary rabbit and mouse α5 antibody incubation at 4°C). Sections were mounted with 1:1 PBS:glycerol containing 0.1% sodium azide, and viewed with a Leica DM5500B wide-field fluorescence photomicroscope with a Hamamatsu Orca Flash 4.0 digital camera. Importantly, several controls were also performed. Firstly, an initial series of staining was performed with only one step of double labeling (overnight primary rabbit and mouse α5 antibody incubation at 4°C) that gave the same overall staining pattern for each antibody as observed with triple labeling. Moreover, normal rabbit serum primary incubations were also performed to ensure the absence of non-specific staining.

For whole-mount labeling, fixed fish were bleached in a solution of 70% ethanol, 1% H_2O_2 for 1 week and were then blocked overnight with 5% normal goat serum in PBS containing 0.1% Triton X-100. Then fish were incubated with rabbit (1:500) and mouse α5 (1:200) antibodies as described above for 24 h followed by a 24-h incubation with secondary antibodies as above (1:500) at room temperature. Samples were viewed with a Leica M165FC fluorescence stereo photomicroscope with a Hamamatsu Orca Flash 4.0 digital camera.

Statistical analyses

All data have been presented as means±s.e.m. (n=sample size). All statistical analyses were performed using SigmaStat v3.5 (Systat

Journal of Experimental Biology (2017) 220, 775-786 doi:10.1242/jeb.148429

Software Inc., San Jose, CA, USA). Significance was accepted at the $P<0.05$ level. In general, statistically significant differences between two means were tested using an unpaired two-tailed Student's *t*-test, whereas comparisons between more than two means were conducted using a one-way ANOVA followed by a Holm–Sidak *post hoc* test. In Series 3, a two-way ANOVA followed by a Holm–Sidak *post hoc* test was used to determine differences among blockers and between control and HEA means. Specific tests used for each data set are explained in detail in corresponding figure captions.

RESULTS

Series 1 – effects of HEA pre-exposure

Pre-exposing CYA trout to 12 h of HEA (0.5 mmol l^{-1} NH_4HCO_3) led to a significant 3-fold increase in branchial (anterior compartment) J_{amm}, measured in ammonia-free water (Fig. 2B), and a nearly 2-fold increase in branchial $J_{Na,in}$ (Fig. 2A). HEA pre-exposure also increased J_{amm} by ~2-fold across the body epithelium (posterior compartment) in CYA fish (Fig. 2B), whereas $J_{Na,in}$ was unchanged (Fig. 2A). Under control conditions, the anterior compartment accounted for 98% and 71% of total $J_{Na,in}$ and J_{amm}, respectively, and these contributions increased to 99% and 80% of total following HEA exposure (Fig. 2).

In the yolk sac epithelium (ventral compartment) of PH fish, HEA pre-exposure caused a ~2-fold increase in J_{amm} across the yolk sac skin (Fig. 2B) with no change in $J_{Na,in}$ (Fig. 2A).

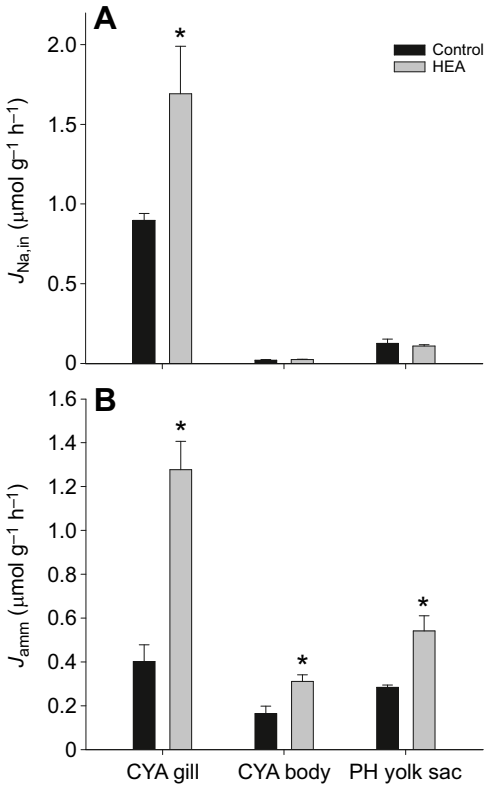

Fig. 2. The effects of high environmental ammonia on sodium uptake and ammonia excretion by the gills, body skin, and yolk sac skin. Sodium uptake (A; $J_{Na,in}$) and ammonia excretion (B; J_{amm}) across the CYA gill, CYA body, and PH yolk sac under control conditions (black bars) and following exposure to 0.5 mmol l^{-1} NH_4HCO_3 for 12 h [high environmental ammonia (HEA); grey bars]. Data are means±s.e.m. Asterisks represent statistically significant differences between control and HEA groups across a given epithelium as determined by a Student's two-tailed *t*-test (n=6–9; $P<0.05$).

Series 2 – gene expression and immunostaining

In response to HEA exposure, mRNA expression of NHE2 and H^+-ATPase increased significantly in the gills of CYA fish, by ~2.5- and 2-fold, respectively (Fig. 3D,G). No significant changes in the expression of any other gene were observed in the CYA gill (Fig. 3). In the body epithelium of CYA trout, HEA had no effect on mRNA expression of any of the examined genes and, moreover, transcripts for Rhcg1, NHE3b and Na^+/K^+-ATPase were below the limit of detection (Fig. 3A,E,F). In the yolk sac epithelium of PH larvae, Rhcg2 mRNA expression increased 3-fold in response to HEA (Fig. 3B), whereas the expression of all other genes was unaffected (Fig. 3).

Gill sections of CYA trout and yolk sac skin sections of PH larvae were immunoreactive for most or all of the antibodies utilized in the present study. Note that we did not find any staining above background for any of the antibodies in the body skin of CYA trout. We also did not find any apparent differences in staining pattern or intensity between control and HEA-exposed fish, thus only representative images from control animals are shown (Figs 4, 5 and 6). Furthermore, two antibodies raised against the V-type H^+-ATPase B subunit [BvA2; Wilson et al., 2007 and B1/2 (H-180) Santa Cruz Biotechnology] were tested but we could not detect immunoreactivity in any tissue.

In the gill, Na^+/K^+-ATPase staining (α5 antibody) was generally restricted to distinct cells in the filament epithelium (Fig. 4Ai,Bi, Ci), although in some instances immunoreactivity was detected in the lamellar epithelial cells (e.g. Fig. 4Di). Whole-cell staining in both filamental and lamellar cells was observed, indicative of ionocyte tubular system staining. Rhcg1 staining (Fig. 4Aii,Bii,Cii) was always localized apically to the cells that stained for Na^+/K^+-ATPase; however, not all Na^+/K^+-ATPase-positive cells expressed Rhcg1 (Fig. 4). Apical Rhcg2 staining was found primarily in gill lamellae, and was never co-localized with Na^+/K^+-ATPase or Rhcg1 staining (Fig. 4Aiii,Av), presumably indicating that this protein is localized to pavement cells. NHE2 (Fig. 4Biii,Bv) and NHE3b (Fig. 4Ciii,v) staining was apically co-localized to Na^+/K^+-ATPase-positive cells, similar to Rhcg1 staining (Fig. 4Bv,Cv). Rhbg staining was ubiquitous throughout the gill filaments and lamellae (Fig. 4Dii). DIC images merged with DAPI staining (Fig. 4Aiv,Biv,Civ,Diii) are also shown. Images in Fig. 4Av,Bv,Cv, Div represent the merged images of preceding panels except that the DIC image was excluded for clearer visualization.

In the yolk sac epithelium of PH larvae, Rhcg1 apical immunostaining was always co-localized with Na^+/K^+-ATPase staining (Fig. 5A–C). Unlike the situation in the gill, however, we were unable to detect Rhcg2 staining in the yolk sac skin of control or HEA-exposed larvae (Fig. 5Aiii). Similarly, staining for NHE2 was not detectable against background fluorescence (Fig. 5Biii). Apical NHE3b staining was localized to Na^+/K^+-ATPase-positive cells, along with Rhcg1 (Fig. 5Cv). Similar to the gill, Rhbg staining was ubiquitous in the yolk sac skin (Fig. 5Dii). As in Fig. 4, DIC images merged with DAPI staining are also shown (Fig. 5Aiv,Biv,Civ,Diii) and images in Fig. 5Av,Bv,Cv,Div represent merged images of preceding panels. Double whole-mount staining of Na^+/K^+-ATPase and Rhcg1 (Fig. 6A) and Na^+/K^+-ATPase and NHE3b (Fig. 6B) further demonstrated that both Rhcg1 and NHE3b are localized to Na^+/K^+-ATPase-positive cells. Similar to the gill, not all Na^+/K^+-ATPase-positive cells in the yolk sac epithelium expressed Rhcg1 and NHE3b. Note that images in Fig. 6A, B were taken from two separate individuals.

Series 3 – effects of pharmacological blockers

In CYA fish, branchial $J_{Na,in}$ was significantly inhibited (85% reduction) by EIPA, relative to DMSO controls, whereas

Journal of Experimental Biology (2017) 220, 775-786 doi:10.1242/jeb.148429

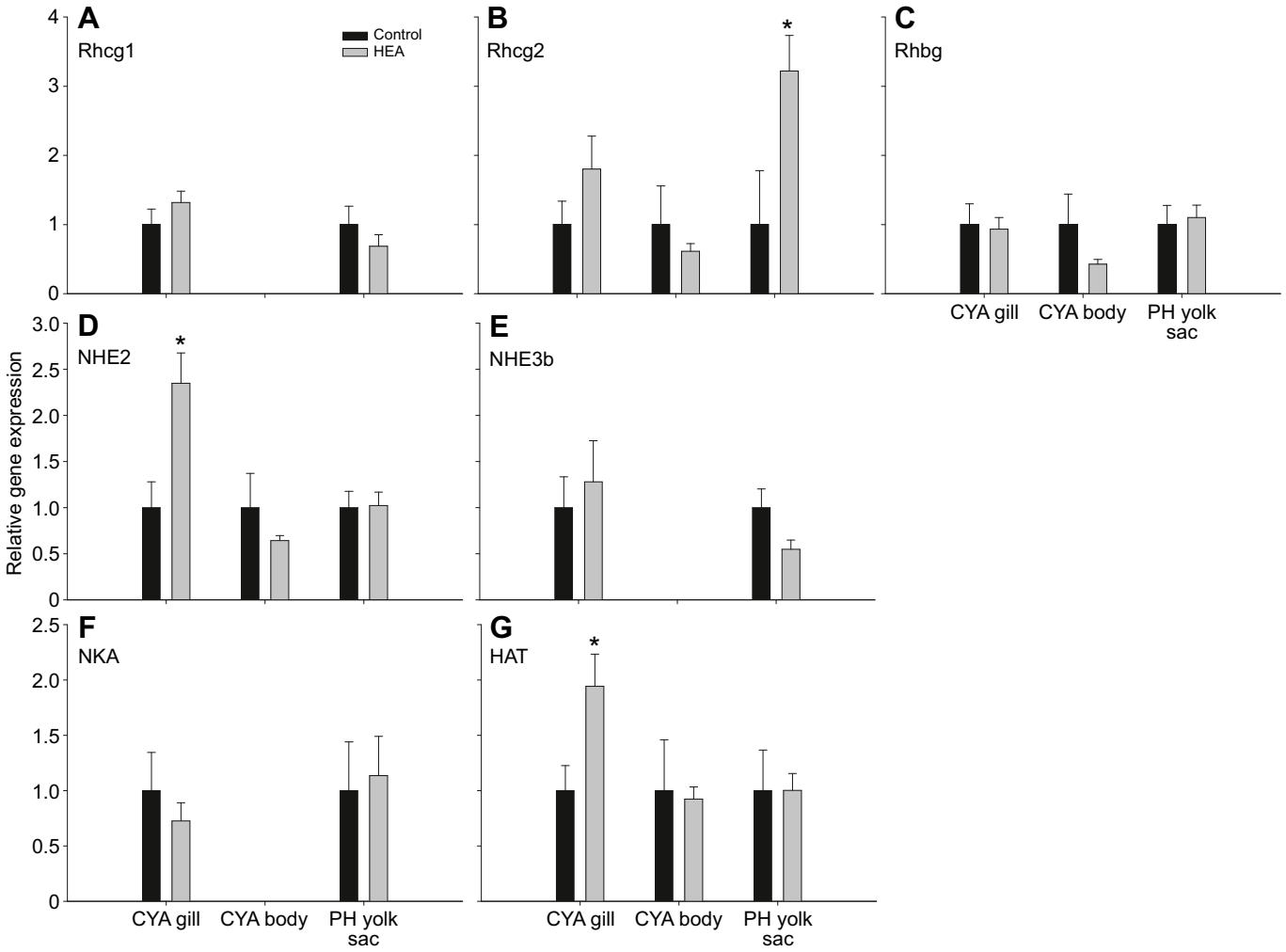

Fig. 3. The effects of high environmental ammonia on gene expression of Na^+/NH_4^+ exchange complex proteins. Relative expression of (A) Rhcg1, (B) Rhcg2, (C) Rhbg, (D) NHE2, (E) NHE3b, (F) Na^+/K^+-ATPase (NKA) and (G) H^+-ATPase (HAT) mRNA following 12-h exposures to control conditions (black bars) or to 0.5 mmol l^{-1} NH_4HCO_3 for 12 h [high environmental ammonia (HEA); grey bars]. Data are means±s.e.m. Asterisks represent statistically significant differences between control and HEA groups within a given tissue as determined by a Student's two-tailed *t*-test. Gene expression was normalized to the geometric mean of EF1α and β-actin and is expressed relative to control means within a given tissue (n=6–9; P<0.05).

bafilomycin and phenamil had no significant effects (Fig. 7A). Branchial J_{amm} in CYA fish was also significantly inhibited by EIPA (Fig. 7B), though these effects (~40% reduction from DMSO controls) were much less than the effects on $J_{Na,in}$. Bafilomycin and phenamil had no significant effect on J_{amm} in these fish (Fig. 7B).

In the presence of DMSO, the increase in $J_{Na,in}$ following HEA exposure was attenuated compared with Series 1 (Fig. 2A) but $J_{Na,in}$ was still significantly elevated relative to control DMSO fish (Fig. 7A). Similar to the situation in control fish, EIPA inhibited $J_{Na,in}$ in HEA-exposed fish by 85%, completely blocking the HEA-induced increase in $J_{Na,in}$ observed in the DMSO control (Fig. 7A). None of the blockers significantly inhibited J_{amm} by HEA-exposed fish (Fig. 7B).

In PH fish, EIPA inhibited $J_{Na,in}$ by the yolk sac skin by ~50% relative to DMSO alone, whereas bafilomycin and phenamil had no significant effects (Fig. 8).

DISCUSSION

Na^+/NH_4^+ exchange by the gill, but not the skin, of rainbow trout

In general, our findings support our hypothesis that $J_{Na,in}$ and J_{amm} occur as loosely coupled Na^+/NH_4^+ exchange at the gills of CYA trout, but not at the yolk sac skin of PH trout. Pre-exposure to 12 h of HEA (0.5 mmol l^{-1} NH_4HCO_3) led to significant increases in $J_{Na,in}$ and J_{amm} by the gills of CYA trout, whereas $J_{Na,in}$ by the body skin of CYA trout or yolk sac skin of PH trout was unaffected, despite the fact that J_{amm} increased significantly across both cutaneous epithelia (Fig. 2). In the present study, we measured fluxes following transfer to control water, as opposed to measuring fluxes in HEA because HEA exposure has been demonstrated to transiently inhibit $J_{Na,in}$ in many fish species (Maetz and Garcia-Romeu, 1964; Avella and Bornancin, 1989; Wilson et al., 1994; Zimmer et al., 2010; Kumai and Perry, 2011; Shih et al., 2012; Liew et al., 2013), likely owing to NH_4^+ cation competition at Na^+ uptake sites. Thus, the increase in $J_{Na,in}$ observed in the present study (Fig. 2A) might have been masked by the inhibitory effect of external NH_4^+ in previous studies. The presence of branchial Na^+/NH_4^+ exchange by the CYA gill was further supported by the increase in gene expression of proteins involved in $J_{Na,in}$ (NHE2 and H^+-ATPase) in the CYA gill in response to HEA, but not in either skin tissue (Fig. 3D,F). The presence of branchial Na^+/NH_4^+ exchange was also supported by treatment with EIPA, which caused significant inhibitions of both $J_{Na,in}$ and J_{amm} by the CYA gill (Fig. 7). Na^+/NH_4^+ exchange by the

Journal of Experimental Biology (2017) 220, 775-786 doi:10.1242/jeb.148429

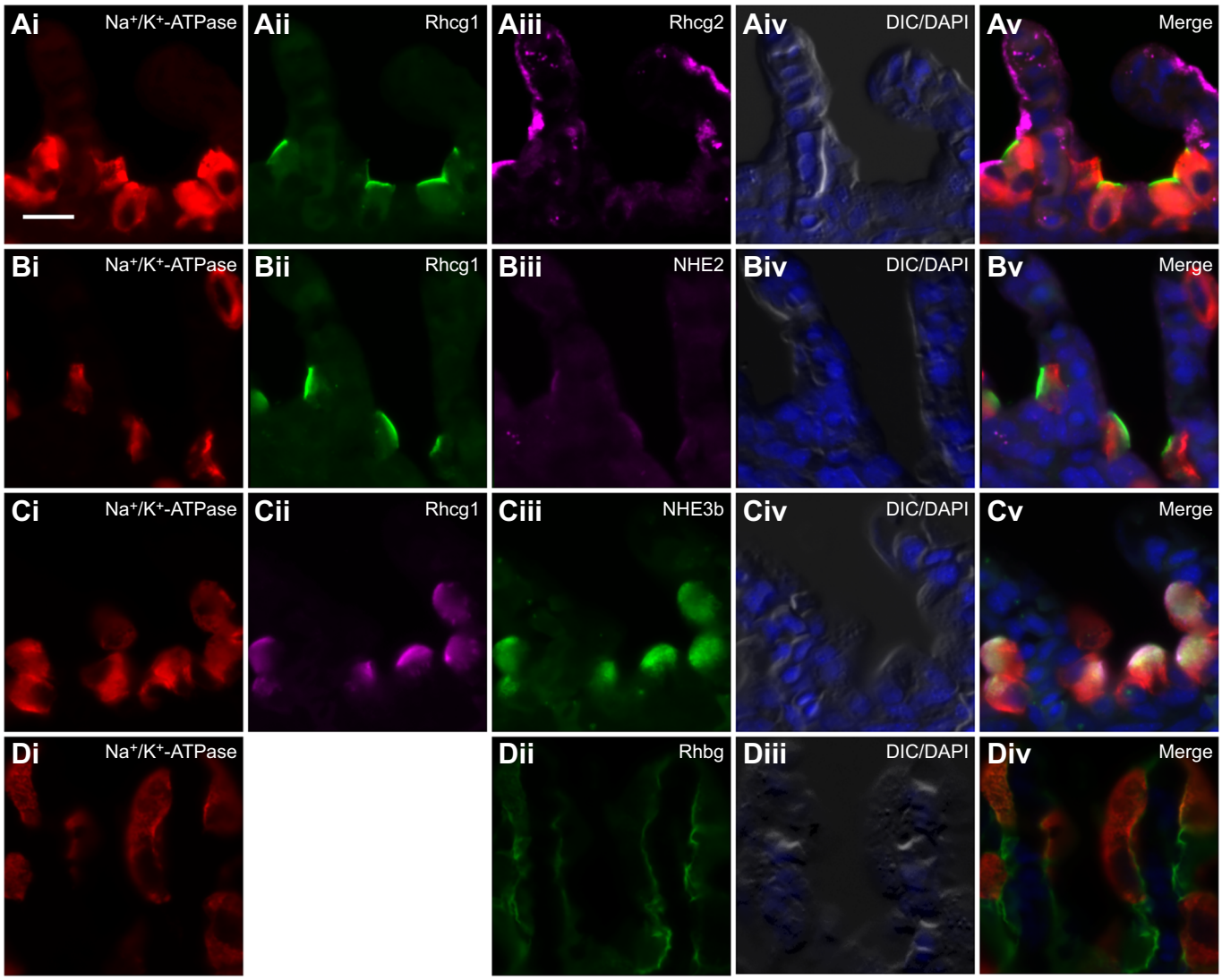

Fig. 4. Immunolocalization of Na^+/NH_4^+ exchange complex proteins in the gills of CYA rainbow trout. Triple immunofluorescent localization of Na^+/K^+-ATPase (Ai,Bi,Ci), Rhcg1 (Aii,Bii,Cii), and either Rhcg2 (Aiii), NHE2 (Biii) or NHE3b (Ciii), and double immunofluorescent localization of Na^+/K^+-ATPase (Di) and Rhbg (Dii) of gill sections from control CYA rainbow trout. Each row of panels represents the same section probed with different antibodies; panels Aiv, Biv, Civ, and Diii are merged DIC images and DAPI staining and panels Av, Bv, Cv, and Div are merged images of all antibodies and DAPI. Scale bar: 10 µm.

gill, and lack thereof by the skin, has also been supported by the tight correlation between branchial $J_{Na,in}$ and J_{amm} over the first 21 days post-hatch in larval trout and the absence of a parallel correlation at the skin (Zimmer et al., 2014c). Similarly, exposure to waterborne Cu^{2+}, a potent inhibitor of $J_{Na,in}$, inhibited both $J_{Na,in}$ and J_{amm} by the gills of late stage larvae, but inhibited only $J_{Na,in}$ by the yolk sac skin of early stage larvae (Zimmer et al., 2014b).

Branchial mechanisms of $J_{Na,in}$ and J_{amm}

The broader goal of the present study was to characterize the mechanisms of $J_{Na,in}$ and J_{amm} utilized by the primary exchange epithelia of developmentally distinct CYA and PH trout. One of the most recent changes in current models for $J_{Na,in}$ by freshwater fish is the inclusion of Rh proteins (Wright and Wood, 2009, 2012; Dymowska et al., 2012). In CYA trout, exposure to 12 h of HEA increased both $J_{Na,in}$ and J_{amm} but did not significantly increase the expression of any Rh paralogues in the gill (Fig. 3A–C). This was surprising as HEA exposure generally increases Rhcg2 mRNA expression in the gills (or isolated gill cells) of juvenile and adult rainbow trout (Nawata et al., 2007; Tsui et al., 2009; Zimmer et al., 2010; Wood and Nawata, 2011; Sinha et al., 2013), suggesting a potential developmental delay in this response given its absence in CYA trout. Branchial gene expression of Rhcg1 is usually not altered by ammonia exposure in adult trout (Nawata et al., 2007; Tsui et al., 2009; Wood and Nawata, 2011; Sinha et al., 2013), in agreement with our findings in CYA trout (Fig. 3A). Nawata et al. (2007) reported that the increase in Rhcg2 mRNA expression typically observed in the gills of adult trout in response to HEA exposure was localized to pavement cells (PVCs), whereas neither Rhcg1 nor Rhcg2 expression was altered in ionocytes. This is in agreement with the pattern of immunostaining of CYA gill sections that localized apical Rhcg2 primarily to gill lamellae (PVCs; Fig. 4Aiii) whereas Rhcg1 was localized to Na^+/K^+-ATPase-positive cells (ionocytes; Fig. 4Aii–Cii).

Although once considered to be a contentious issue on a thermodynamic basis (Parks et al., 2008), the involvement of NHEs in $J_{Na,in}$ by freshwater fish has since been solidified (Kumai and Perry, 2011; Shih et al., 2012; Ito et al., 2013; Boyle et al., 2016). In

Journal of Experimental Biology (2017) 220, 775-786 doi:10.1242/jeb.148429

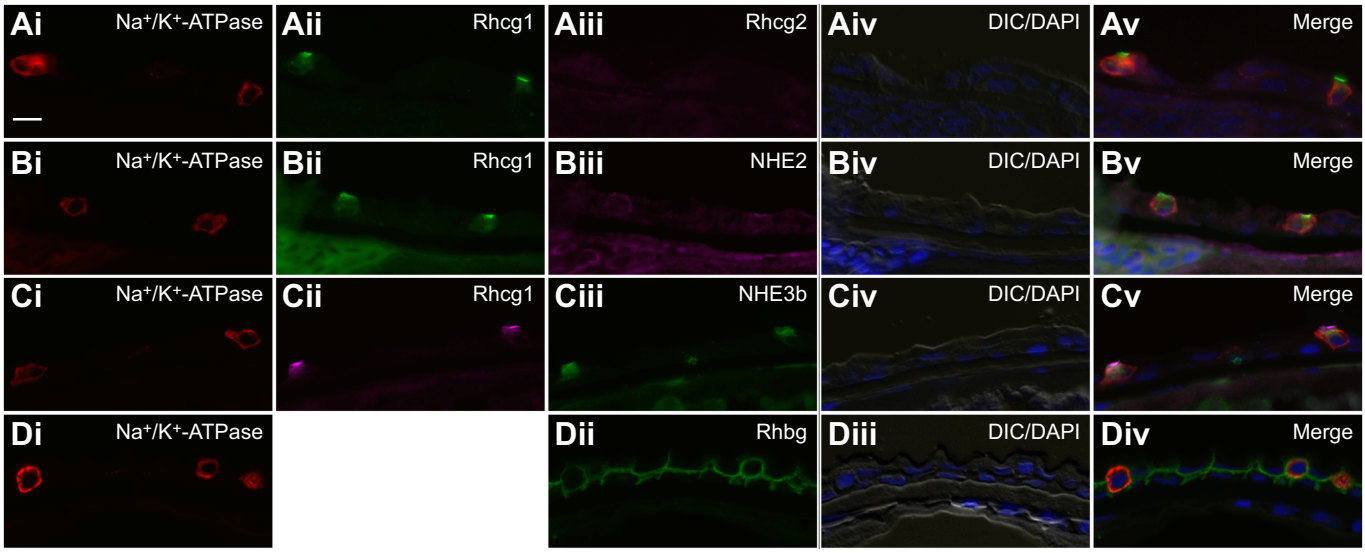

Fig. 5. Immunolocalization of Na^+/NH_4^+ exchange complex proteins in the yolk sac epithelium of PH rainbow trout. Triple immunofluorescent localization of Na^+/K^+-ATPase (Ai,Bi,Ci), Rhcg1 (Aii,Bii,Cii), and either Rhcg2 (Aiii), NHE2 (Biii) or NHE3b (Ciii), and double immunofluorescent localization of Na^+/K^+-ATPase (Di) and Rhbg (Dii) of yolk sac sections from control PH rainbow trout. Each row of panels represents the same section probed with different antibodies; panels Aiv, Biv, Civ, and Diii are merged DIC images and DAPI staining and panels Av, Bv, Cv, and Div are merged images of all antibodies and DAPI. Scale bar: 10 µm.

CYA trout, the increase in $J_{Na,in}$ following HEA exposure was accompanied by an increase in gill NHE2 (but not NHE3b) gene expression (Fig. 3D,E). Upregulation of NHE gene expression in response to HEA has been demonstrated repeatedly in juvenile and adult trout (Tsui et al., 2009; Zimmer et al., 2010; Wood and Nawata, 2011; Sinha et al., 2013), although absent in at least one study (Nawata et al., 2007), and has also been shown to be specific to NHE2 and not NHE3b (Wood and Nawata, 2011). In contrast, recent work demonstrated that when developing trout were acclimated to soft water with low $[Na^+]$, NHE3b, but not NHE2, gene expression increased significantly and this increase was accompanied by an increase in $J_{Na,in}$ (Boyle et al., 2016). In adult trout, hypercapnic acidosis significantly increased NHE2 mRNA expression, but not NHE3b mRNA expression, in the gills of adult trout (Ivanis et al., 2008). These results point to potential paralog-specific responses of NHE genes to different environmental challenges in trout that certainly warrants further investigation. A similar role for NHE3 in the acclimation to low $[Na^+]$ conditions has also been demonstrated in zebrafish (Shih et al., 2012), Japanese medaka (*Oryzias latipes*; Wu et al., 2010), and pupfish (*Cyprinodon variegatus variegatus* and *Cyprinodon variegatus hubbsi*; Brix et al., 2014).

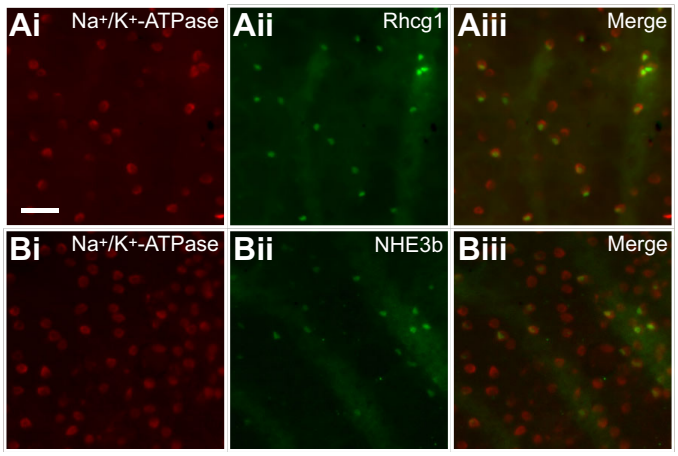

Fig. 6. Whole-mount immunostaining of Na^+/K^+-ATPase, NHE3b and Rhcg1 on the surface of the yolk sac of PH rainbow trout. Double immunofluorescent whole-mount staining of Na^+/K^+-ATPase (Ai,Bi) and Rhcg1 (Aii) or NHE3b (Bii) on the surface of the yolk sac epithelium of PH trout. Each row of panels represents the same fixed larva probed with different antibodies; panels Aiii and Biii are merged images of both antibodies. Scale bar: 50 µm.

In the gills of adult trout, both NHE isoforms are localized to PNA^+ ionocytes (Ivanis et al., 2008). In gill sections from CYA trout, NHE2 and NHE3b seemed to co-localize apically to Na^+/K^+-ATPase-positive cells, which also expressed apical Rhcg1 (Fig. 4B,C). Thus, we propose that PNA^+ ionocytes, in addition to NHE2/3b, also express Rhcg1. A role for NHEs in branchial Na^+/NH_4^+ exchange was further demonstrated using EIPA, which inhibited $J_{Na,in}$ by 85%, similar to recent work in larval trout (Boyle et al., 2016), and simultaneously inhibited J_{amm} by 40% (Fig. 7). Moreover, following exposure to HEA, EIPA treatment completely blocked the increase in $J_{Na,in}$, suggesting that NHE (potentially NHE2, based on the response at the gene level) is crucial to Na^+/NH_4^+ exchange coupling in the relatively high $[Na^+]$/high pH water used in our study. The fact that EIPA had no effect on J_{amm} following HEA exposure illustrates the flexible nature of the Na^+/NH_4^+ exchange complex system. Treatment of adult rainbow trout with amiloride, a non-specific Na^+ uptake blocker, similarly had large inhibitory effects on $J_{Na,in}$ but comparatively smaller inhibitory effects on J_{amm} (Payan, 1978; Wilson et al., 1994). This inhibitory effect of EIPA (and amiloride) on J_{amm} under control conditions is most likely explained by a decrease in boundary layer acidification.

In addition to loose Rh–NHE coupling, H^+-ATPase also contributes mechanistically to both $J_{Na,in}$ and J_{amm}, and can be considered another component of the overall metabolon (Wright and Wood, 2009, 2012). In trout, bafilomycin and phenamil (blockers of H^+-ATPase and Na^+ channels, respectively) have been reported to inhibit $J_{Na,in}$ in both *in vivo* and *in vitro* tests (Bury and Wood, 1999; Grosell and Wood, 2002; Reid et al., 2003; Rogers et al., 2005; Goss et al., 2011). In contrast, we found that

Journal of Experimental Biology (2017) 220, 775-786 doi:10.1242/jeb.148429

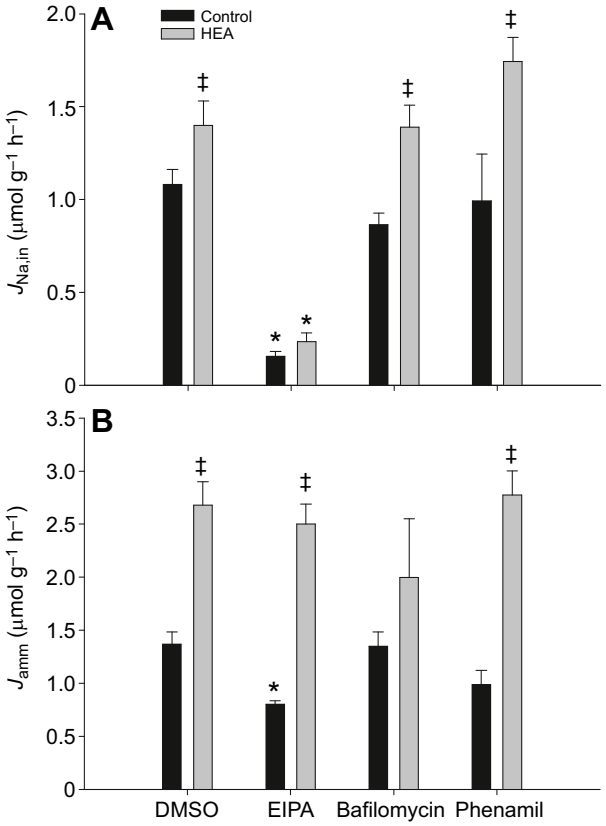

Fig. 7. Effects of pharmacological blockers on Na^+ uptake and ammonia excretion by the gills of CYA rainbow trout. Na^+ uptake (A; $J_{Na,in}$) and ammonia excretion (B; J_{amm}) across the CYA gill in response to DMSO (0.1% vehicle control) and to the pharmacological blockers EIPA (1×10^{-4} mol l^{-1}), bafilomycin (5×10^{-6} mol l^{-1}), and phenamil (1×10^{-4} mol l^{-1}) dissolved in 0.1% DMSO following 12-h exposures to control conditions (black bars) or high environmental ammonia (HEA; 0.5 mmol l^{-1} NH_4HCO_3; grey bars). Data are means±s.e.m. Asterisks represent statistically significant differences from the DMSO value and daggers represent significant effects of HEA pre-exposure as determined by a two-way ANOVA followed by a Holm–Sidak *post hoc* test (n=4–9; P<0.05). There was no significant interaction between both factors (P=0.129).

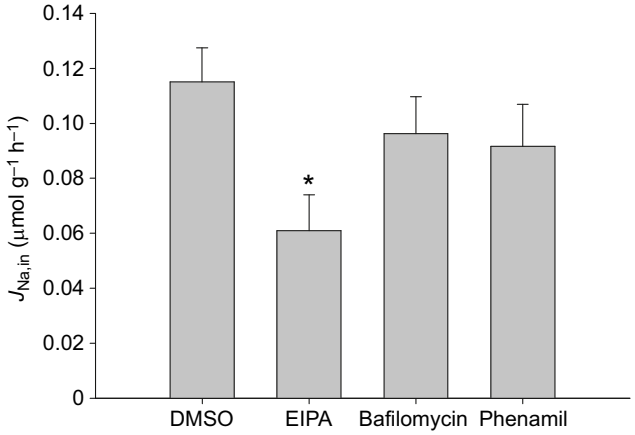

Fig. 8. Effects of pharmacological blockers on Na^+ uptake by the yolk sac epithelium of PH rainbow trout. Na^+ uptake ($J_{Na,in}$) across the PH yolk sac epithelium in response to DMSO (0.1% vehicle control) and to the pharmacological blockers EIPA (1×10^{-4} mol l^{-1}), bafilomycin (5×10^{-6} mol l^{-1}), and phenamil (1×10^{-4} mol l^{-1}) dissolved in 0.1% DMSO. Data are means± s.e.m. Asterisk represents statistically significant difference from the DMSO value as determined by a one-way ANOVA followed by a Holm–Sidak *post hoc* test (n=6–14; P<0.05).

bafilomycin and phenamil had no effects on $J_{Na,in}$. Given that these blockers have been demonstrated to inhibit $J_{Na,in}$ in several studies, we cannot discount the role of H^+-ATPase and a putative Na^+ channel in overall branchial $J_{Na,in}$ by CYA trout. Moreover, recent evidence has suggested that this putative Na^+ channel might be an acid-sensing ion channel (ASIC; Dymowska et al., 2014, 2015) that is DAPI-sensitive and not affected by phenamil.

The increase in H^+-ATPase gene expression in the gill of CYA trout in response to HEA exposure further suggests a role for H^+-ATPase in Na^+/NH_4^+ exchange (Fig. 3F), and has been reported repeatedly in juvenile and adult trout (Nawata et al., 2007; Tsui et al., 2009; Zimmer et al., 2010; Wood and Nawata, 2011; Sinha et al., 2013). Nawata et al. (2007) demonstrated that this increased gene expression was specific to PVCs, similar to the response of Rhcg2 mRNA expression to HEA exposure. Although we were unable to visualize H^+-ATPase by immunohistochemistry to validate the possible co-localization of H^+-ATPase and Rhcg2 in branchial PVCs, earlier work has shown immunostaining of H^+-ATPase in both ionocytes and PVCs (Lin et al., 1994; Sullivan et al., 1995; Wilson et al., 2000). Bafilomycin treatment also had no effect on J_{amm}, unlike previous *in vitro* work in isolated gill cells of adult trout (Tsui et al., 2009). Perhaps H^+-ATPase is recruited to enhance J_{amm} primarily when active excretion against a gradient is required, playing a minimal role in control (or post-HEA exposure) conditions.

Overall, we propose that the major site of functional Na^+/NH_4^+ exchange in the CYA gill is the putative PNA^+ ionocyte, whereas putative PNA^- ionocytes and PVCs likely represent important sites of uncoupled $J_{Na,in}$ and J_{amm}, respectively (Fig. 9A). In our model, PNA^+ ionocytes express basolateral Na^+/K^+-ATPase and apical Rhcg1, NHE2, NHE3b and possibly H^+-ATPase. Recent models suggest that H^+-ATPase is localized specifically to PNA^- ionocytes (Dymowska et al., 2012); however, H^+-ATPase protein expression was only twofold higher in PNA^- ionocytes relative to PNA^+ ionocytes (Galvez et al., 2002) and both cell types exhibited bafilomycin-sensitive $J_{Na,in}$ *in vitro* (Reid et al., 2003). Further studies are needed to understand H^+-ATPase function in all three cell types (PNA^+ ionocyte, PNA^- ionocyte and PVC). Based on the co-localization of Rhcg1 and NHEs (Fig. 4), PNA^- ionocytes likely do not express apical Rhcg1 or Rhcg2 and might serve primarily for Na^+/H^+ exchange via H^+-ATPase and a putative Na^+ channel (Reid et al., 2003), which might be an ASIC (Dymowska et al., 2014). Finally, PVCs are likely important sites for J_{amm} via Rhcg2, and H^+-ATPase might be involved in active ammonia excretion by these cells (Nawata et al., 2007). This model for the CYA gill of trout is summarized in Fig. 9A. Notably, this model is very similar to that proposed for the gills of juvenile and adult rainbow trout (Wright and Wood, 2009; Dymowska et al., 2012). The only major mechanistic difference we observed between the gills of CYA and juvenile or adult trout was a lack of Rhcg2 mRNA upregulation in response to HEA exposure (Fig. 3B), which we have interpreted as a developmental delay. In our proposed model, all cell types likely express basolateral Rhbg, based on ubiquitous staining of gill lamellae and filaments (Fig. 4Dii), which has been observed previously in trout (J.H., unpublished results). However, the function of Rhbg in PNA^- ionocytes is unclear at present.

Cutaneous mechanisms of $J_{Na,in}$ and J_{amm}

J_{amm} by the PH yolk sac skin increased significantly upon exposure to HEA, in conjunction with a significant increase in Rhcg2 mRNA

Journal of Experimental Biology (2017) 220, 775-786 doi:10.1242/jeb.148429

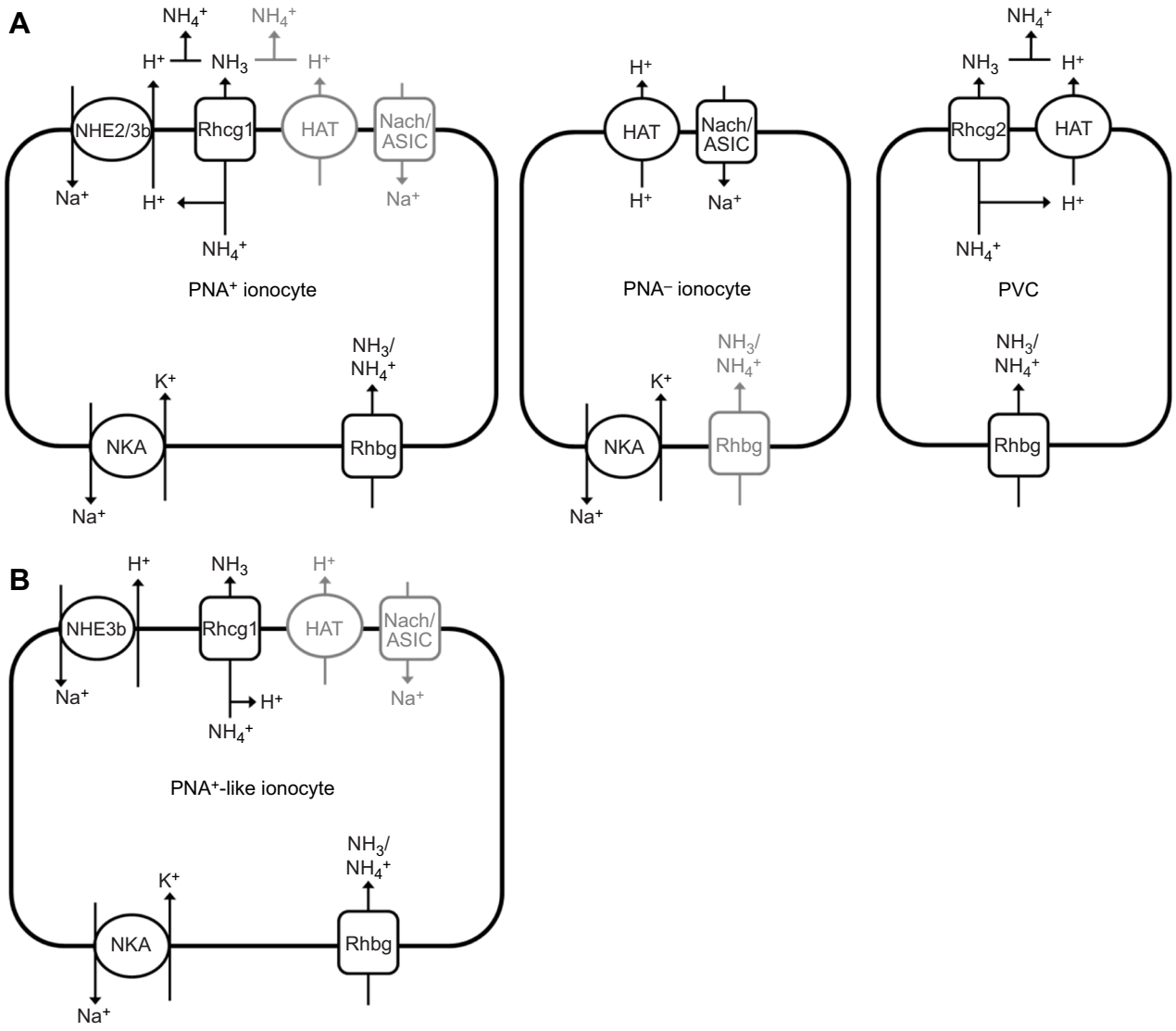

Fig. 9. Proposed mechanistic models for $J_{Na,in}$ and J_{amm} by gill cells and yolk sac epithelium cells. Cellular models of $J_{Na,in}$ and J_{amm} by (A) gill and (B) yolk sac skin cell types. Components shaded in grey are those that remain unclear. See text for further details. ASIC, acid-sensing ion channel; NaCh, putative epithelial channel; HAT, H^+-ATPase; NKA, Na^+/K^+-ATPase; NHE, Na^+/H^+-exchanger proteins; PNA, peanut lectin agglutinin; PVC, pavement cell; Rh, Rhesus proteins.

expression in this tissue (Fig. 2B, Fig. 3B). J_{amm} by the body skin of CYA trout also increased following HEA exposure, similar to a previous report in adult trout (Zimmer et al., 2014a), but Rh gene expression did not change (Fig. 3A–C). In adult trout, some studies report an increase in Rh gene expression in the skin during HEA exposure (Nawata et al., 2007), whereas others do not (Nawata and Wood, 2008; Zimmer et al., 2014a). Thus, more work is needed to determine what role, if any, Rh proteins play in facilitating J_{amm} across the body skin of CYA and adult trout.

In zebrafish larvae, Rhcg1 facilitates J_{amm} by the yolk sac epithelium under high $[Na^+]$/high pH conditions ($[Na^+]$=0.5–0.8 mmol l^{-1}; pH 7–8) (Shih et al., 2008; Braun et al., 2009) but participates in the coordination of $J_{Na,in}$ only under low pH (pH 4) or low $[Na^+]$ (0.05 mmol l^{-1}) rearing conditions (Kumai and Perry, 2011; Shih et al., 2012). Under high $[Na^+]$/high pH conditions, coupled Na^+/NH_4^+ exchange mediated by the Rh–NHE metabolon is absent (Kumai and Perry, 2011; Shih et al., 2012). Similar to the situation in zebrafish, $J_{Na,in}$ by the yolk sac skin of PH trout is not coupled to J_{amm} under high $[Na^+]$/high pH rearing conditions, as indicated by the lack of HEA-induced increase in $J_{Na,in}$ (Fig. 2A). The reason for this lack of coupling, compared with branchial Na^+/NH_4^+ exchange observed in CYA (present study) and adult trout is not clear. The yolk sac epithelium possesses Na^+/K^+-ATPase-positive cells that express apical Rhcg1 and NHE3b (Fig. 5, Fig. 6A). However, we were unable to detect Rhcg2 or NHE2 protein expression by immunohistochemistry in yolk sac sections from control or HEA-exposed PH larvae (Fig. 5Aiii), despite the fact that Rhcg2 gene expression in this tissue increased in response to HEA exposure (Fig. 3B). This might indicate that the expression of Rhcg2 protein was below the limit of detection for immunohistochemical techniques. In future studies, it will be informative to determine the localization of Rhcg2 in the yolk sac skin in order to characterize the ammonia-transporting cell types present in this epithelium. We have identified at least one cell type that expresses apical Rhcg1 and thus likely plays a role in J_{amm} by the yolk sac skin of PH larvae (Fig. 5, Fig. 6A).

We propose that the Na^+/K^+-ATPase-positive cells in the yolk sac epithelium that express apical Rhcg1 and NHE3b might share similar properties to branchial PNA^+ ionocytes described here (Fig. 9A) and elsewhere (Dymowska et al., 2012) and thus we have identified these cells as PNA^+-like ionocytes. The presence of this NHE3b-expressing ionocyte in the yolk sac skin is in agreement with an important role for NHE3b in larval trout in responding to soft water acclimation ($[Na^+]$=0.1 mmol l^{-1}) relative to fish reared in hard water ($[Na^+]$=2.2 mmol l^{-1}) (Boyle et al., 2016). A major difference between PNA^+-like cutaneous ionocytes and branchial PNA^+ ionocytes is the absence of NHE2 immunostaining (Fig. 5Biii). Moreover, expression of NHE2 mRNA in the PH yolk sac skin was not altered by exposure to HEA (Fig. 3D). This difference could potentially account for the lack of coupled Na^+/NH_4^+ exchange by the yolk sac epithelium, given that increased branchial NHE2 gene expression is a potential hallmark of HEA exposure in trout (Fig. 3D) (Tsui et al., 2009; Zimmer et al., 2010; Wood and Nawata, 2011; Sinha et al., 2013). Nevertheless, some isoform of NHE does contribute substantially to Na^+ uptake by the yolk sac epithelium of trout as EIPA inhibited $J_{Na,in}$ by 50% (Fig. 8), in agreement with previous work in PH trout (Boyle et al., 2016). Note that this lack of coupled Na^+/NH_4^+ exchange by the yolk sac epithelium under high $[Na^+]$/high pH conditions observed in PH trout and larval zebrafish (e.g. Kumai and Perry, 2011) is not universal. In larval Japanese medaka, Na^+/NH_4^+ exchange is present under high $[Na^+]$/high pH rearing conditions (Wu et al., 2010).

Bafilomycin and phenamil had no substantial effects on $J_{Na,in}$ by the yolk sac skin of PH trout, similar to the CYA gill. This is again in contrast with previous studies that have shown that both of these blockers inhibited $J_{Na,in}$ in whole rainbow trout alevins of similar size and at similar concentrations (Bury and Wood, 1999; Grosell and Wood, 2002; Rogers et al., 2005). Notably, in two of these studies (Bury and Wood, 1999; Grosell and Wood, 2002) fish were acclimated to soft water ($[Na^+]$=0.05 mmol l^{-1}; pH 6), which might account for the differences from our study. A tentative model for $J_{Na,in}$ and J_{amm} by PNA^+-like ionocytes in the yolk sac epithelium of PH trout is presented in Fig. 9B; we propose that these cells also express basolateral Rhbg, based on the ubiquitous staining observed in this epithelium.

Conclusion

In conclusion, we have provided evidence demonstrating that the mechanisms of $J_{Na,in}$ and J_{amm} by the gills of CYA trout and yolk sac skin of PH trout, the dominant sites of these fluxes at two distinct developmental stages, differ substantially in early life. Our findings suggest that a lack of NHE2 expression in the yolk sac epithelium might be the underlying difference, resulting in a lack of Na^+/NH_4^+ exchange by the skin. This observation is novel and highlights the importance of a developmental approach to ionoregulatory physiology.

Acknowledgements

The authors wish to thank Dr Michele Nawata for helpful advice and insight into qPCR protocols and Justine Doherty for assistance with immunolabeling. We also extend our gratitude to Dr Steve Perry (University of Ottawa, Ottawa, Canada) for providing trout NHE2 antibodies.

Competing interests

The authors declare no competing or financial interests.

Author contributions

A.M.Z. performed all experiments and analyses and drafted the initial manuscript. J.H. provided antibodies for immunolabeling and contributed advice and insight into immunolabeling approaches. P.A.W. contributed to the design of the study and experiments. J.M.W. assisted in all immunolabeling procedures. C.M.W. contributed to the overall conception of the study, and the design of all experiments. All authors edited the manuscript.

Funding

This research was funded by a Natural Sciences and Engineering Research Council of Canada (NSERC) Discovery Grant (RGPIN473-12) to C.M.W.

References

Avella, M. and Bornancin, M. (1989). A new analysis of ammonia and sodium transport through the gills of the freshwater rainbow trout (*Salmo gairdneri*). *J. Exp. Biol.* **142**, 155-175.

Boyle, D., Blair, S. D., Chamot, D. and Goss, G. G. (2016). Characterization of developmental Na^+ uptake in rainbow trout larvae supports a significant role for Nhe3b. *Comp. Biochem. Physiol. A Mol. Integr. Physiol.* **201**, 30-36.

Braun, M. H., Steele, S. L., Ekker, M. and Perry, S. F. (2009). Nitrogen excretion in developing zebrafish (*Danio rerio*): a role for Rh proteins and urea transporters. *Am. J. Physiol. Renal Physiol.* **296**, F994-F1005.

Brix, K. V., Esbaugh, A. J., Mager, E. M. and Grosell, M. (2014). Comparative evaluation of Na^+ uptake in *Cyprinodon variegatus variegatus* (Lacepede) and *Cyprinodon variegatus hubbsi* (Carr) (Cyprinodontiformes, Teleostei): evaluation of NHE function in high and low Na^+ freshwater. *Comp. Biochem. Physiol. A Mol. Integr. Physiol.* **185**, 115-124.

Bury, N. R. and Wood, C. M. (1999). Mechanism of branchial apical silver uptake by rainbow trout is via the proton-coupled Na^+ channel. *Am. J. Physiol. Regul. Integr. Comp. Physiol.* **277**, R1385-R1391.

Cameron, J. N. and Heisler, N. (1983). Studies of ammonia in the rainbow trout: Physico-chemical parameters, acid-base behaviour and respiratory clearance. *J. Exp. Biol.* **105**, 107-125.

Caner, T., Abdulnour-Nakhoul, S., Brown, K., Islam, M. T., Hamm, L. L. and Nakhoul, N. L. (2015). Mechanisms of ammonia and ammonium transport by rhesus associated glycoproteins. *Am. J. Physiol. Cell Physiol.* **309**, C747-C758.

Dymowska, A. K., Hwang, P.-P. and Goss, G. G. (2012). Structure and function of ionocytes in the freshwater fish gill. *Respir. Physiol. Neurobiol.* **184**, 282-292.

Dymowska, A. K., Boyle, D., Schultz, A. G. and Goss, G. (2015). The role of acid-sensing ion channels in epithelial Na^+ uptake in adult zebrafish (*Danio rerio*). *J. Exp. Biol.* **218**, 1244-1251.

Dymowska, A. K., Schultz, A. G., Blair, S. D., Chamot, D. and Goss, G. G. (2014). Acid-sensing ion channels are involved in epithelial Na^+ uptake in the rainbow trout *Oncorhynchus mykiss*. *Am. J. Physiol. Cell Physiol.* **307**, C255-C265.

Esaki, M., Hoshijima, K., Kobayashi, S., Fukuda, H., Kawakami, K. and Hirose, S. (2007). Visualization in zebrafish larvae of Na^+ uptake in mitochondria-rich cells whose differentiation is dependent on foxi3a. *Am. J. Physiol. Regul. Integr. Comp. Physiol.* **292**, R470-R480.

Fu, C., Wilson, J. M., Rombough, P. J. and Brauner, C. J. (2010). Ions first: Na^+ uptake shifts from the skin to the gills before O_2 uptake in developing rainbow trout, *Oncorhynchus mykiss*. *Proc. R. Soc. B Biol. Sci.* **277**, 1553-1560.

Galvez, F., Reid, S. D., Hawkings, G. and Goss, G. G. (2002). Isolation and characterization of mitochondria-rich cell types from the gill of freshwater rainbow trout. *Am. J. Physiol. Regul. Integr. Comp. Physiol.* **282**, R658-R668.

Goss, G., Gilmour, K., Hawkings, G., Brumbach, J. H., Huynh, M. and Galvez, F. (2011). Mechanism of sodium uptake in PNA negative MR cells from rainbow trout, *Oncorhynchus mykiss* as revealed by silver and copper inhibition. *Comp. Biochem. Physiol. A Mol. Integr. Physiol.* **159**, 234-241.

Grosell, M. and Wood, C. M. (2002). Copper uptake across rainbow trout gills: mechanisms of apical entry. *J. Exp. Biol.* **205**, 1179-1188.

Hung, C. C., Nawata, C. M., Wood, C. M. and Wright, P. A. (2008). Rhesus glycoprotein and urea transporter genes are expressed in early stages of development of rainbow trout (*Oncorhynchus mykiss*). *J. Exp. Zool. A Ecol. Genet. Physiol.* **309A**, 262-268.

Ip, Y. K. and Chew, S. F. (2010). Ammonia production, excretion, toxicity, and defense in fish: a review. *Front. Physiol.* **1**, 134.

Ito, Y., Kobayashi, S., Nakamura, N., Miyagi, H., Esaki, M., Hoshijima, K. and Hirose, S. (2013). Close association of carbonic anhydrase (CA2a and CA15a), Na^+/H^+ exchanger (Nhe3b), and ammonia transporter Rhcg1 in zebrafish ionocytes responsible for Na^+ uptake. *Front. Physiol.* **4**, 59.

Ivanis, G., Esbaugh, A. J. and Perry, S. F. (2008). Branchial expression and localization of SLC9A2 and SLC9A3 sodium/hydrogen exchangers and their possible role in acid-base regulation in freshwater rainbow trout (*Oncorhynchus mykiss*). *J. Exp. Biol.* **211**, 2467-2477.

Krogh, A. (1939). *Osmotic Regulation in Aquatic Animals*. Cambridge: Cambridge University Press.

Kumai, Y. and Perry, S. F. (2011). Ammonia excretion via Rhcg1 facilitates Na^+ uptake in larval zebrafish, *Danio rerio*, in acidic water. *Am. J. Physiol. Regul. Integr. Comp. Physiol.* **301**, R1517-R1528.

Liew, H. J., Sinha, A. K., Nawata, C. M., Blust, R., Wood, C. M. and De Boeck, G. (2013). Differential responses in ammonia excretion, sodium fluxes and gill permeability explain different sensitivities to acute high environmental ammonia in three freshwater teleosts. *Aquat. Toxicol.* **126**, 63-76.

Lin, H., Pfeiffer, D., Vogl, A., Pan, J. and Randall, D. (1994). Immunolocalization of H^+-ATPase in the gill epithelia of rainbow trout. *J. Exp. Biol.* **195**, 169-183.
Lin, L.-Y., Horng, J.-L., Kunkel, J. G. and Hwang, P.-P. (2006). Proton pump-rich cell secretes acid in skin of zebrafish larvae. *Am. J. Physiol. Cell Physiol.* **290**, C371-C378.
Maetz, J. and Garcia-Romeu, F. (1964). The mechanism of sodium and chloride uptake by the gills of a fresh-water fish, *Carassius auratus*: II. Evidence for NH_4^+/Na^+ and HCO_3^-/Cl^- exchanges. *J. Gen. Physiol.* **47**, 1209.
McFarland, W. N. (1959). A study of the effects of anesthetics on the behaviour and physiology of fishes. *Publ. Inst. Mar. Sci. Univ. Tex.* **6**, 23-55.
Nakada, T., Westhoff, C. M., Kato, A. and Hirose, S. (2007a). Ammonia secretion from fish gill depends on a set of Rh glycoproteins. *FASEB J.* **21**, 1067-1074.
Nawata, C. M. and Wood, C. M. (2008). The effects of CO_2 and external buffering on ammonia excretion and Rhesus glycoprotein mRNA expression in rainbow trout. *J. Exp. Biol.* **211**, 3226-3236.
Nawata, C. M., Hung, C. C. Y., Tsui, T. K. N., Wilson, J. M., Wright, P. A. and Wood, C. M. (2007). Ammonia excretion in rainbow trout (*Oncorhynchus mykiss*): evidence for Rh glycoprotein and H^+-ATPase involvement. *Physiol. Genomics* **31**, 463-474.
Nawata, C. M., Wood, C. M. and O'Donnell, M. J. (2010). Functional characterization of Rhesus glycoproteins from an ammoniotelic teleost, the rainbow trout, using oocyte expression and SIET analysis. *J. Exp. Biol.* **213**, 1049-1059.
Parks, S. K., Tresguerres, M. and Goss, G. G. (2008). Theoretical considerations underlying Na^+ uptake mechanisms in freshwater fishes. *Comp. Biochem. Physiol. C Toxicol. Pharmacol.* **148**, 411-418.
Payan, P. (1978). A study of the Na^+/NH_4^+ exchange across the gill of the perfused head of the trout (*Salmo gairdneri*). *J. Comp. Physiol. B* **124**, 181-188.
Reid, S. D., Hawkings, G. S., Galis, F. and Goss, G. G. (2003). Localization and characterization of phenamil-sensitive Na^+ influx in isolated rainbow trout gill epithelial cells. *J. Exp. Biol.* **206**, 551-559.
Rogers, J. T., Patel, M., Gilmour, K. M. and Wood, C. M. (2005). Mechanisms behind Pb-induced disruption of Na^+ and Cl^- balance in rainbow trout (*Oncorhynchus mykiss*). *Am. J. Physiol. Regul. Integr. Comp. Physiol.* **289**, R463-R472.
Shih, T.-H., Horng, J.-L., Hwang, P.-P. and Lin, L.-Y. (2008). Ammonia excretion by the skin of zebrafish (*Danio rerio*) larvae. *Am. J. Physiol. Cell Physiol.* **295**, C1625-C1632.
Shih, T.-H., Horng, J.-L., Liu, S.-T., Hwang, P.-P. and Lin, L.-Y. (2012). Rhcg1 and NHE3b are involved in ammonium-dependent sodium uptake by zebrafish larvae acclimated to low-sodium water. *Am. J. Physiol. Regul. Integr. Comp. Physiol.* **302**, R84-R93.
Sinha, A. K., Liew, H. J., Nawata, C. M., Blust, R., Wood, C. M. and De Boeck, G. (2013). Modulation of Rh glycoproteins, ammonia excretion and Na^+ fluxes in three freshwater teleosts when exposed chronically to high environmental ammonia. *J. Exp. Biol.* **216**, 2917-2930.
Smith, H. W. (1929). The excretion of ammonia and urea by the gills of fish. *J. Biol. Chem.* **81**, 727-742.
Smith, A. A., Zimmer, A. M. and Wood, C. M. (2012). Branchial and extra-branchial ammonia excretion in goldfish (*Carassius auratus*) following thermally induced gill remodeling. *Comp. Biochem. Physiol. A Mol. Integr. Physiol.* **162**, 185-192.
Sullivan, G., Fryer, J. and Perry, S. (1995). Immunolocalization of proton pumps (H^+-ATPase) in pavement cells of rainbow trout gill. *J. Exp. Biol.* **198**, 2619-2629.
Takeyasu, K., Tamkun, M. M., Renaud, K. J. and Fambrough, D. M. (1988). Ouabain-sensitive (Na^+/K^+)-ATPase activity expressed in mouse L cells by transfection with DNA encoding the alpha-subunit of an avian sodium pump. *J. Biol.Chem.* **263**, 4347-4354.
Tsui, T. K. N., Hung, C. Y. C., Nawata, C. M., Wilson, J. M., Wright, P. A. and Wood, C. M. (2009). Ammonia transport in cultured gill epithelium of freshwater rainbow trout: the importance of Rhesus glycoproteins and the presence of an apical Na^+/NH_4^+ exchange complex. *J. Exp. Biol.* **212**, 878-892.
Verdouw, H., Van Echteld, C. J. A. and Dekkers, E. M. J. (1978). Ammonia determination based on indophenol formation with sodium salicylate. *Water Res.* **12**, 399-402.
Weihrauch, D., Wilkie, M. P. and Walsh, P. J. (2009). Ammonia and urea transporters in gills of fish and aquatic crustaceans. *J. Exp. Biol.* **212**, 2879-2879.
Wilkie, M. P. (1997). Mechanisms of ammonia excretion across fish gills. *Comp. Biochem. Physiol. A Physiol.* **118**, 39-50.
Wilkie, M. P. (2002). Ammonia excretion and urea handling by fish gills: present understanding and future research challenges. *J. Exp. Zool.* **293**, 284-301.
Wilson, R. W., Wright, P. M., Munger, S. and Wood, C. M. (1994). Ammonia excretion in freshwater rainbow trout (*Oncorhynchus mykiss*) and the importance of gill boundary layer acidification: Lack of evidence for Na^+/NH_4^+ exchange. *J. Exp. Biol.* **191**, 37-58.
Wilson, J. M., Laurent, P., Tufts, B. L., Benos, D. J., Donowitz, M., Vogl, A. W. and Randall, D. J. (2000). NaCl uptake by the branchial epithelium in freshwater teleost fish: an immunological approach to ion-transport protein localization. *J. Exp. Biol.* **203**, 2279-2296.
Wilson, J. M., Leitão, A., Gonçalves, A. F., Ferreira, C., Reis-Santos, P., Fonseca, A.-V., da Silva, J. M., Antunes, J. C., Pereira-Wilson, C. and Coimbra, J. (2007). Modulation of branchial ion transport protein expression by salinity in glass eels (*Anguilla anguilla* L.). *Mar. Biol.* **151**, 1633-1645.
Wood, C. M. and Nawata, C. M. (2011). A nose-to-nose comparison of the physiological and molecular responses of rainbow trout to high environmental ammonia in seawater versus freshwater. *J. Exp. Biol.* **214**, 3557-3569.
Wright, P. A. and Wood, C. M. (1985). An analysis of branchial ammonia excretion in the freshwater rainbow trout: effects of environmental pH change and sodium uptake blockade. *J. Exp. Biol.* **114**, 329-353.
Wright, P. A. and Wood, C. M. (2009). A new paradigm for ammonia excretion in aquatic animals: role of Rhesus (Rh) glycoproteins. *J. Exp. Biol.* **212**, 2303-2312.
Wright, P. A. and Wood, C. M. (2012). Seven things fish know about ammonia and we don't. *Respir. Physiol. Neurobiol.* **184**, 231-240.
Wu, S.-C., Horng, J.-L., Liu, S.-T., Hwang, P.-P., Wen, Z.-H., Lin, C.-S. and Lin, L.-Y. (2010). Ammonium-dependent sodium uptake in mitochondrion-rich cells of medaka (*Oryzias latipes*) larvae. *Am. J. Physiol. Cell Physiol.* **298**, C237-C250.
Zimmer, A. M. and Wood, C. M. (2015). Ammonia first? The transition from cutaneous to branchial ammonia excretion in developing rainbow trout is not altered by exposure to chronically high NaCl. *J. Exp. Biol.* **218**, 1467-1470.
Zimmer, A. M., Nawata, C. M. and Wood, C. M. (2010). Physiological and molecular analysis of the interactive effects of feeding and high environmental ammonia on branchial ammonia excretion and Na^+ uptake in freshwater rainbow trout. *J. Comp. Physiol. B* **180**, 1191-1204.
Zimmer, A. M., Brauner, C. J. and Wood, C. M. (2014a). Ammonia transport across the skin of adult rainbow trout (*Oncorhynchus mykiss*) exposed to high environmental ammonia (HEA). *J. Comp. Physiol. B* **184**, 77-90.
Zimmer, A. M., Brauner, C. J. and Wood, C. M. (2014b). Exposure to waterborne Cu inhibits cutaneous Na^+ uptake in post-hatch larval rainbow trout (*Oncorhynchus mykiss*). *Aquat. Toxicol.* **150**, 151-158.
Zimmer, A. M., Wright, P. A. and Wood, C. M. (2014c). What is the primary function of the early teleost gill? Evidence for Na^+/NH_4^+ exchange in developing rainbow trout (*Oncorhynchus mykiss*). *Proc. R. Soc. B Biol. Sci.* **281**, 20141422.

Journal of Experimental Biology